

1
2
3
4
5
6
7
8
9
10
11
12
13
14
15
16
17
18
19
20
21
22
23
24
25
26
27
28

Electronic Supplementary Information

Synthesis of Nanostructured Catalysts by Surfactant-Templating of Large-Pore Zeolites

Aqeel Al-Ani^{a,b}, Josiah J. C. Haslam^a, Natalie E. Mordvinova^c, Oleg I. Lebedev^c, Aurélie Vicente^d, Christian Fernandez^d and Vladimir Zholobenko^{a*}*

^a School of Chemical and Physical Sciences, Keele University, Keele, Staffordshire, ST5 5BG, United Kingdom

^b Oil Marketing Company (SOMO), Baghdad, Iraq

^c Laboratoire CRISMAT ENSICAEN UMR CNRS 6508, 6 Boulevard du Maréchal Juin, 14050, Caen Cedex 04, France

^d Normandie Univ, ENSICAEN, UNICAEN, CNRS, Laboratoire Catalyse et Spectrochimie, 14000 Caen, France

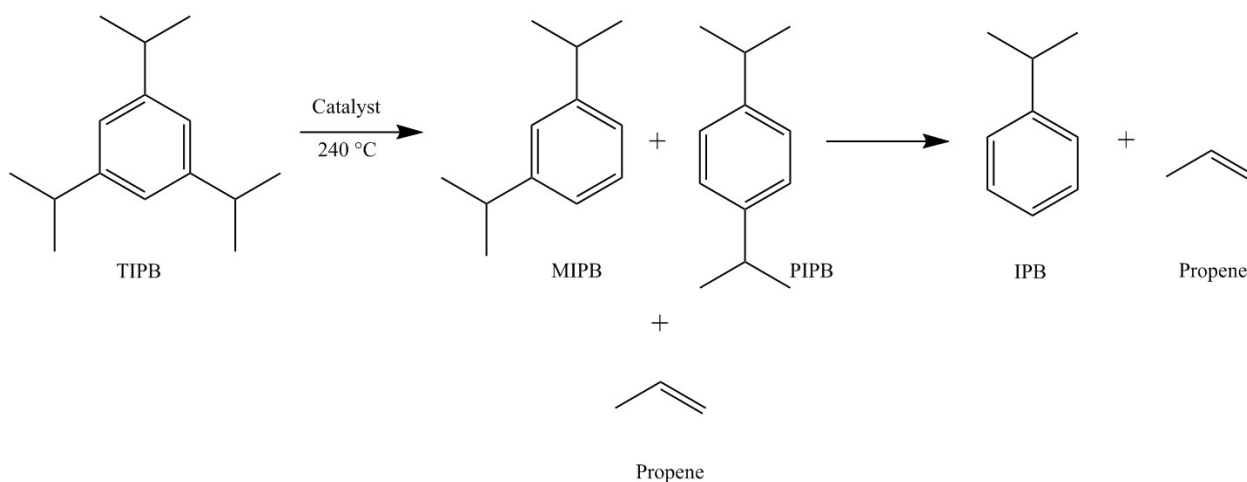
* Corresponding authors:

Aqeel Al-Ani, e-mail address: a.a.t.al-ani@keele.ac.uk

V. Zholobenko, e-mail address: v.l.zholobenko@keele.ac.uk

30 Experimental section

31 The catalytic studies, utilising 1,3,5-tri-isopropylbenzene (TIPB) dealkylation as a reaction test (Ref.
32 S1), were carried out in a conventionally heated high-pressure reaction system, Monowave-50
33 supplied by Anton Paar, using specially designed 10-ml glass vials as batch reactors operating at
34 elevated temperature and pressures (up to 250°C and 20 bar).



35

36 0.2 g of the zeolite catalyst was activated in an open reactor at 400°C for 5 h, cooled down to
37 ~100°C and then mixed with 2 mL of TIPB. The reactor was purged with nitrogen and sealed, the
38 temperature was raised to 240°C (the temperature ramp was ~ 40 °C/min) and kept for 1 h. Next, the
39 reaction mixture was cooled down to ~0°C and the liquid products were isolated and identified using
40 an Agilent 7890A GC with the 5975C mass detection system equipped with a capillary column
41 BPX90 SGE, 15m×0.25mm×0.25µm (1 % solution of the products in MTBE with 0.1 v% of nonane
42 as the internal standard).

43

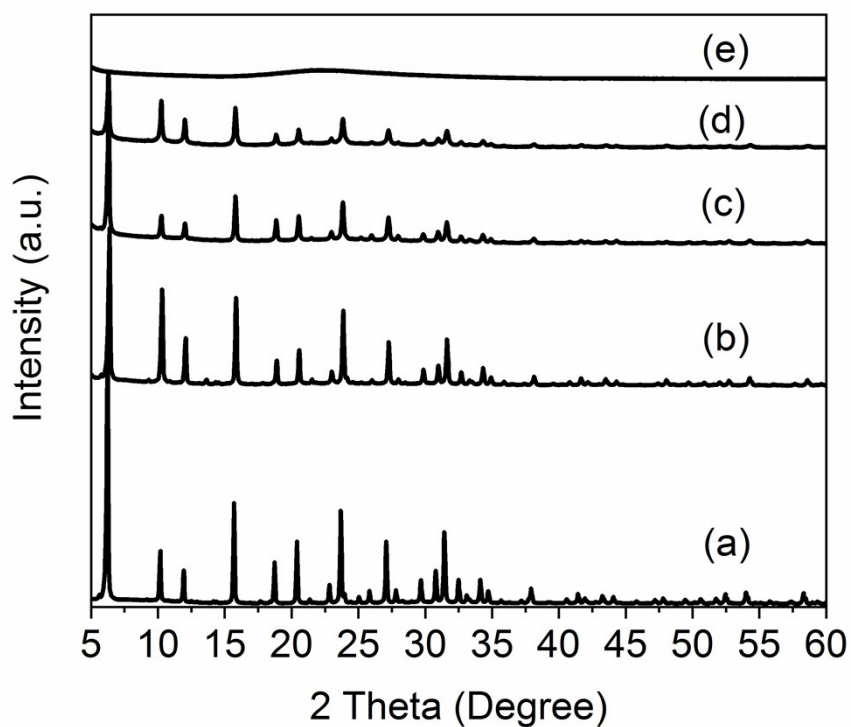
Table S1. GC-MS analysis conditions.

Split ratio	100
Carrier gas	Helium at 1 ml/min
Column temperature	50°C for 3 min 25°C/min to 300°C Hold at 300°C for 2 min
Injector and detector temperature	250°C
Injection volume	0.2 µL

44

45 (S) Qin, Z.; Cychosz, K.A.; Melinte, G.; El Siblani, H.; Gilson, J-P.; Thommes, M.; Fernandez, C.;
46 Mintova, S.; Ersen, O.; Valtchev, V. Opening the Cages of Faujasite-Type Zeolite. *J Am Chem Soc*,
47 **2017**,139,17273-17276.

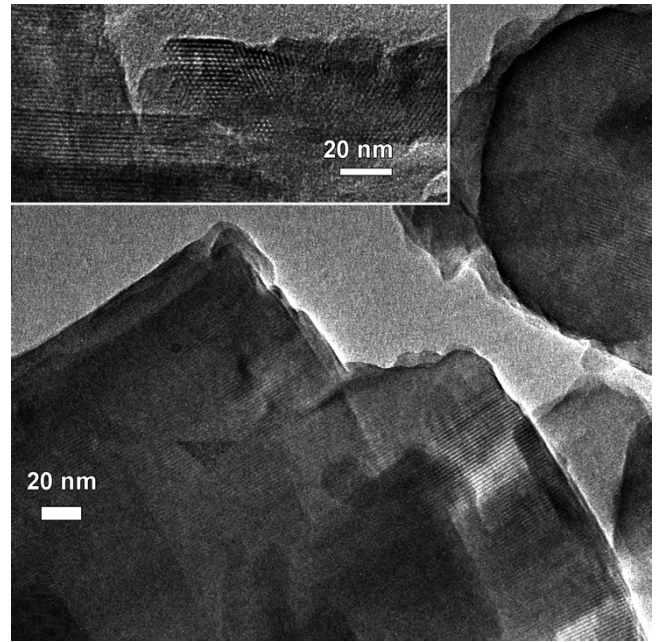
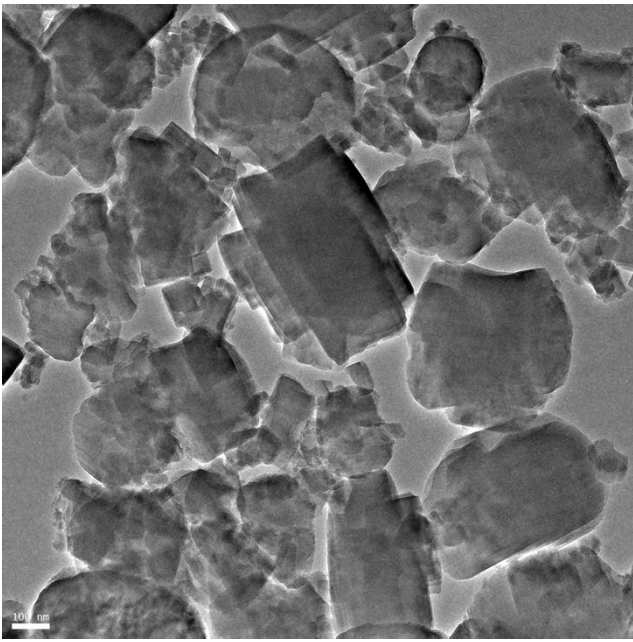
48



49

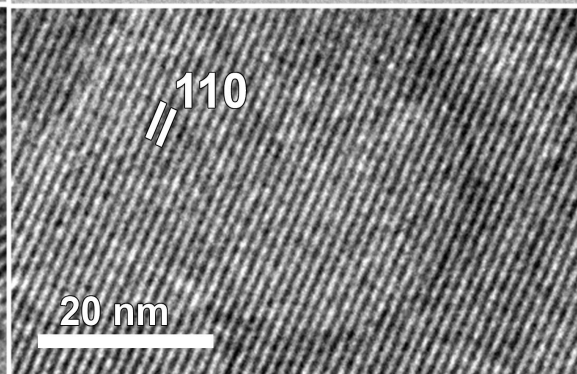
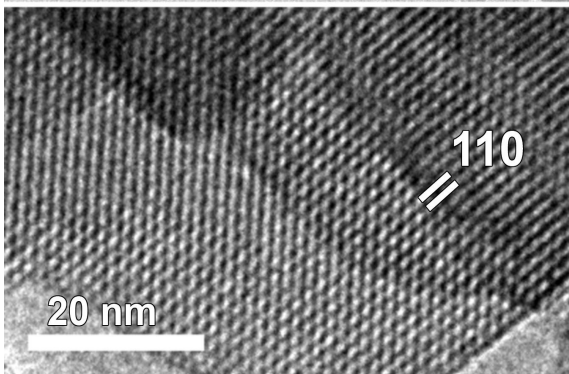
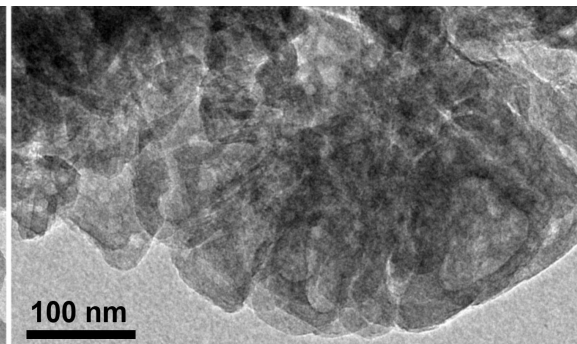
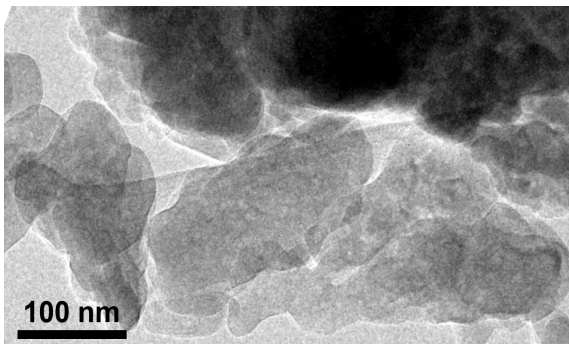
50 **Figure S1.** XRD patterns of faujasite-type zeolites treated with different amount of citric acid (a) 0
51 meq, (b) 4.5 meq, (c) 6 meq, (d) 9 meq and (e) 12 meq.

52 (a)

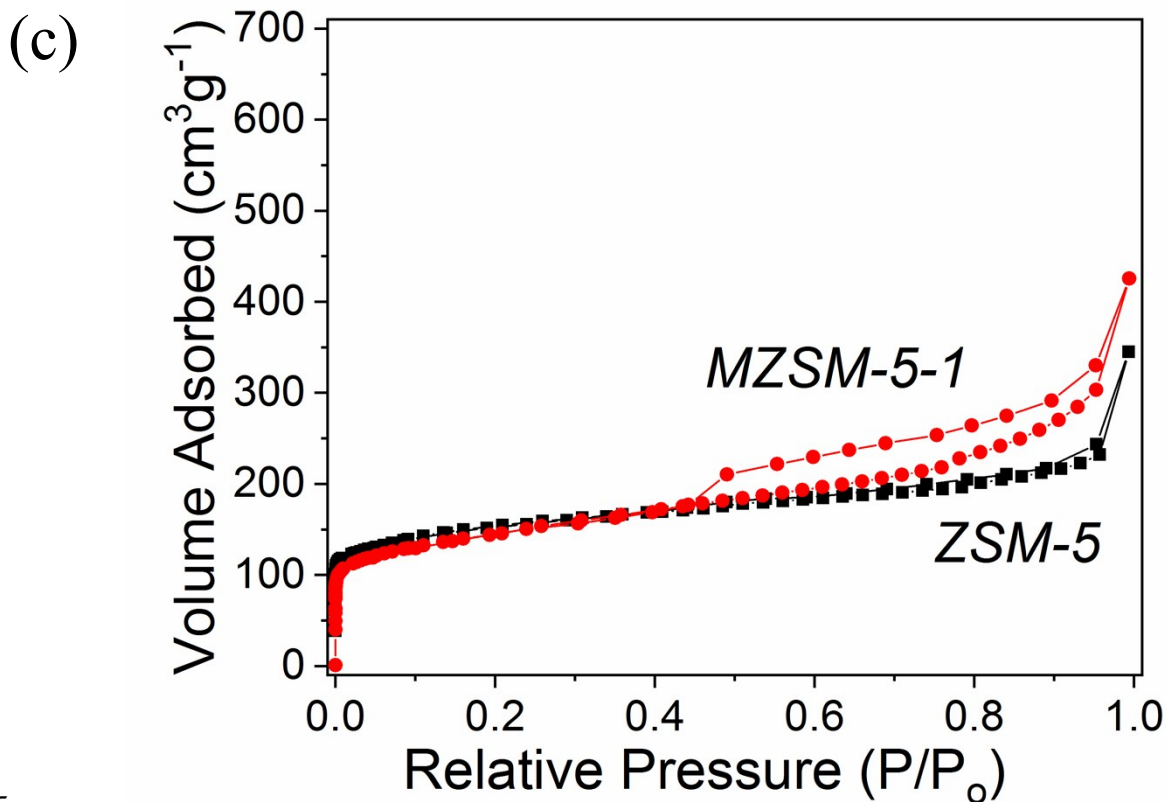


53

(b)

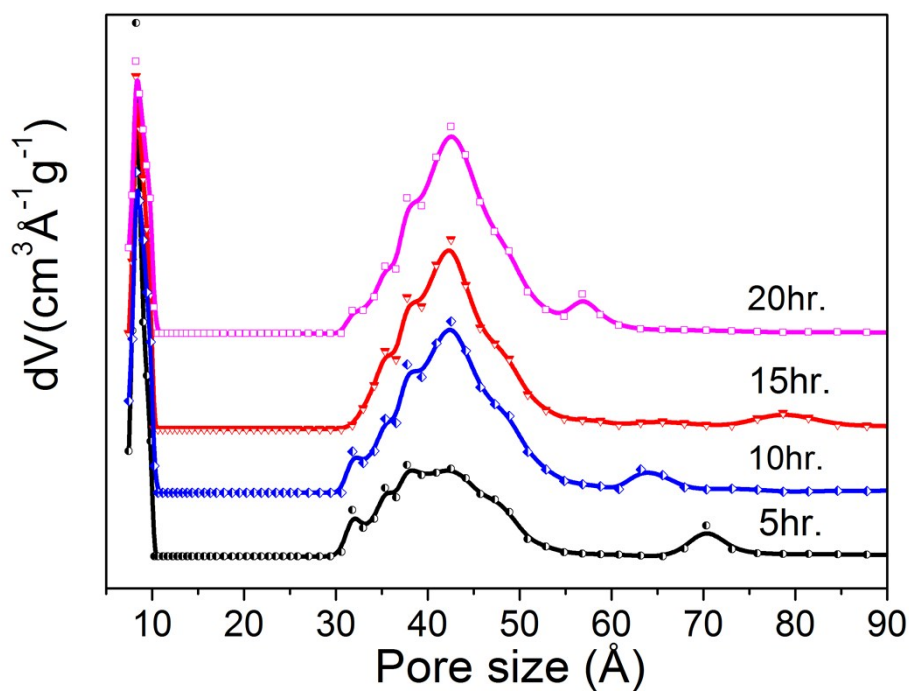


54



55

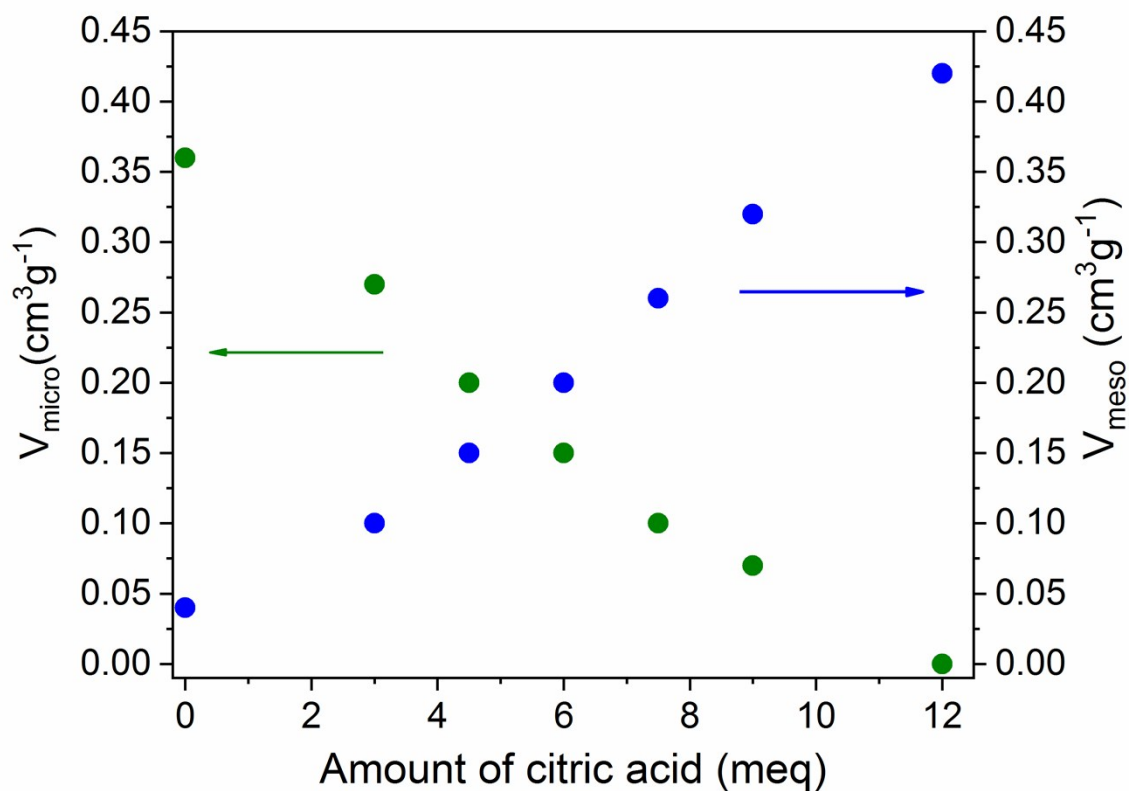
56 **Figure S2.** (a) Bright field TEM images for the parent LTL zeolite; (b) TEM images of the parent
 57 ZSM-5 (left) and mesostructured MZSM-5-1 (right); (c) N_2 adsorption and desorption isotherms for
 58 parent and modified ZSM-5 zeolites.



59

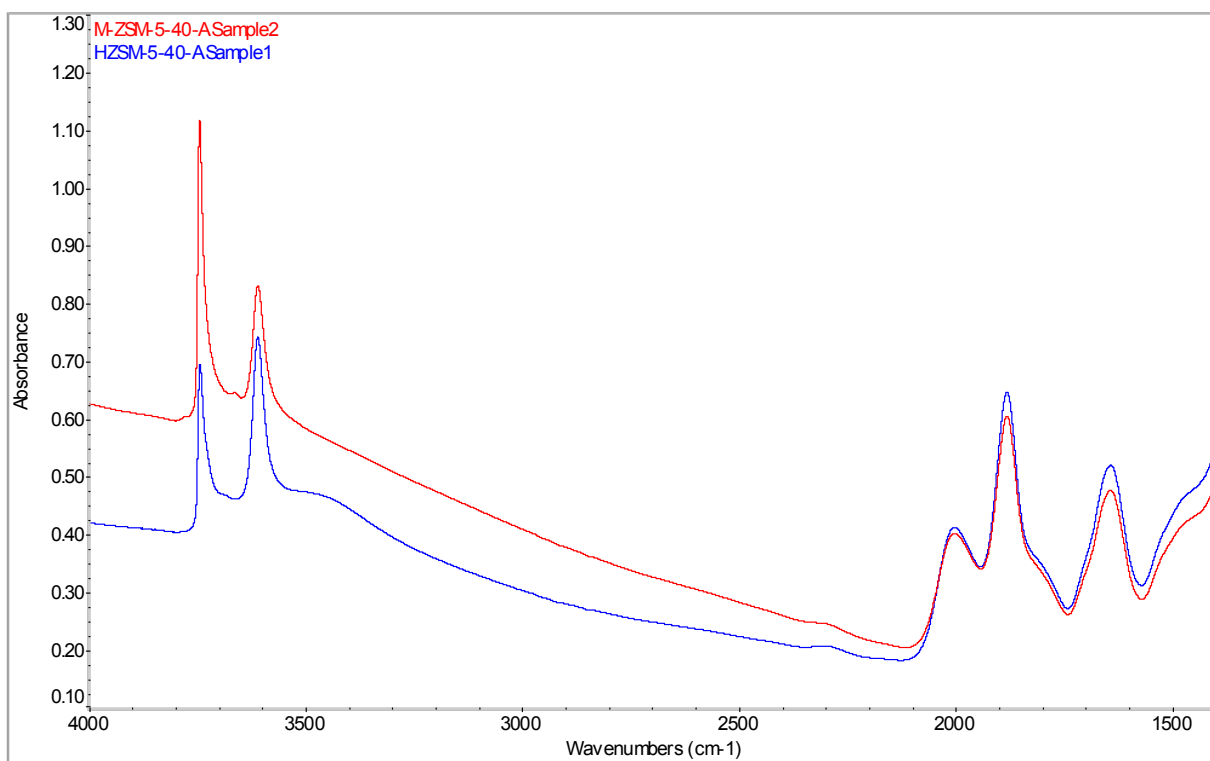
60

Figure S3. Pore size distribution of treated MOR at different times.

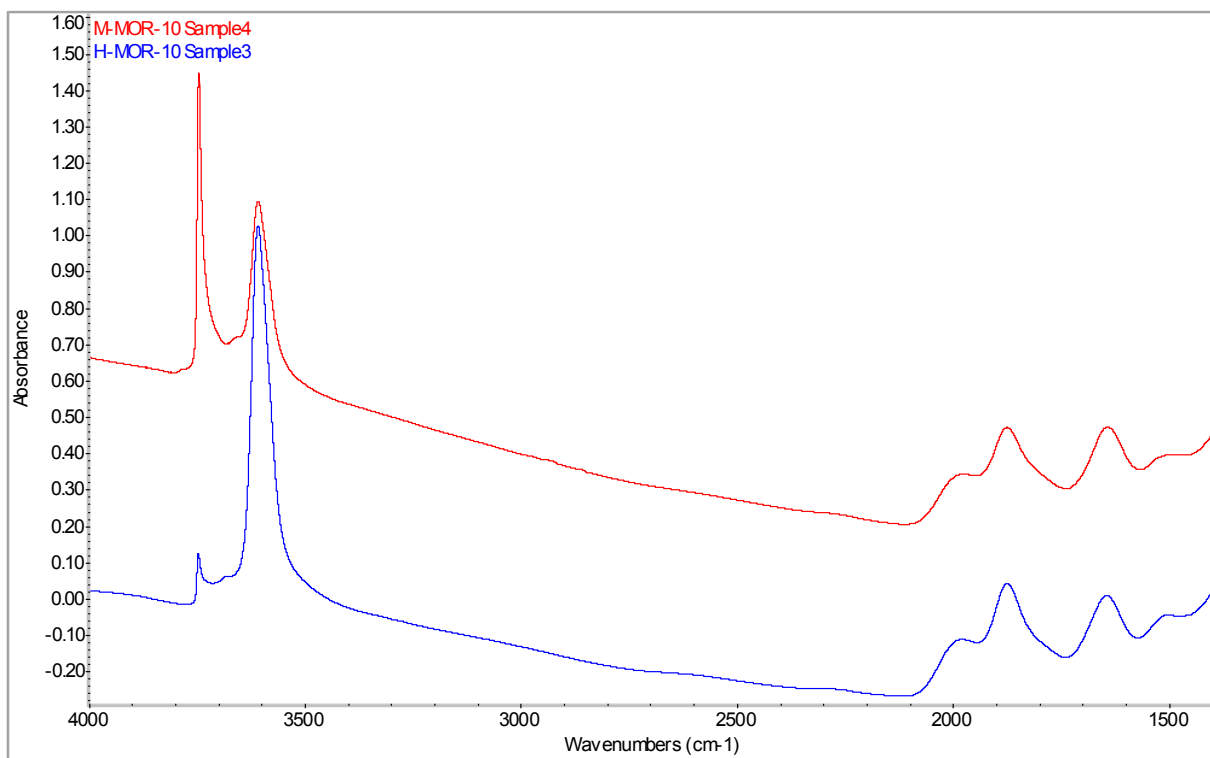


61
 62 **Figure S4.** The relationship between the amount of citric acid added and the pore volume of
 63 modified faujasite-type zeolite.

64

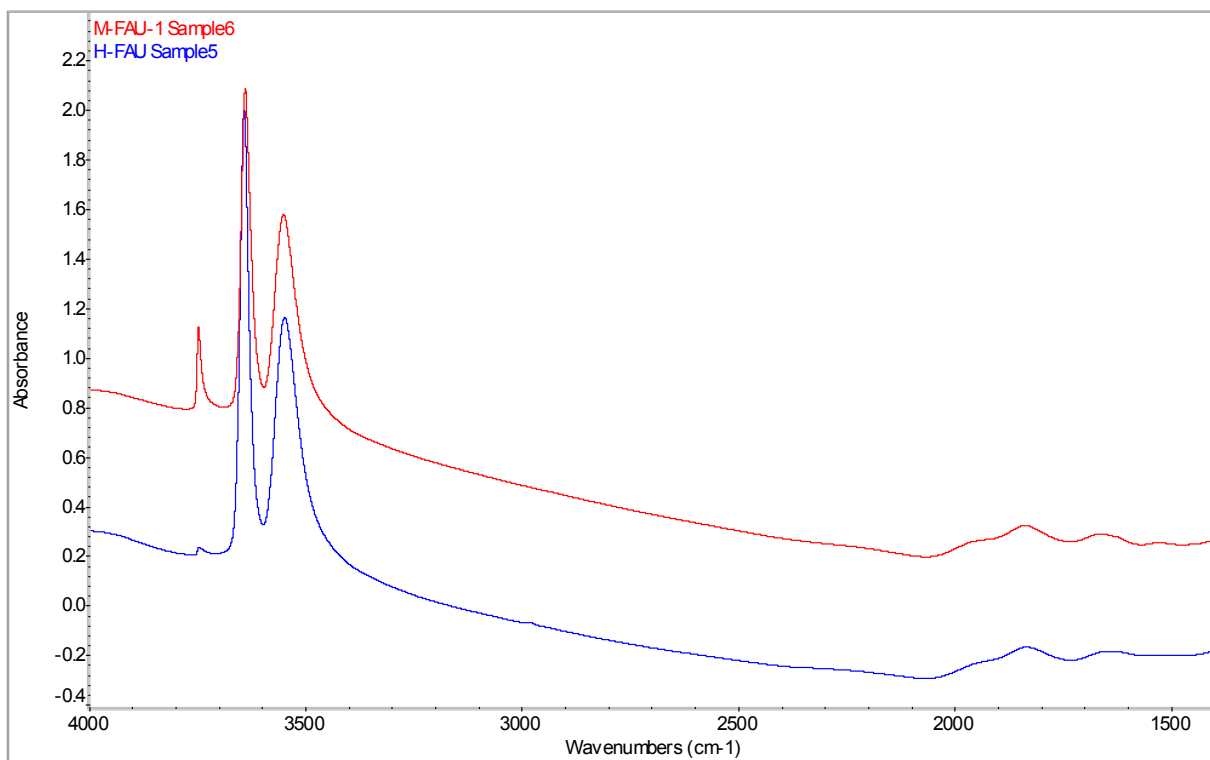


65
 66 **Figure S5a.** FTIR spectra of the O-H region of the parent (blue) and mesostructured (red) ZSM-5.

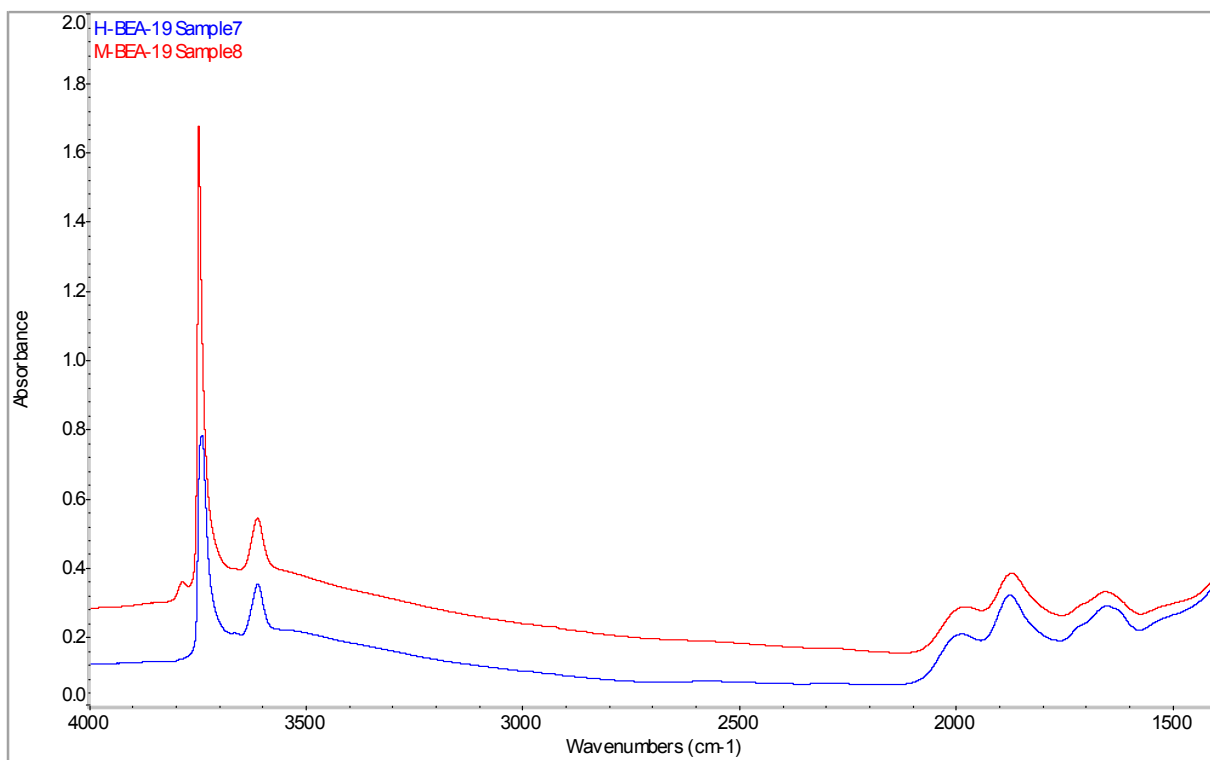


67
 68 **Figure S5b.** FTIR spectra of the O-H region of the **parent (blue)** and **mesostructured (red)** MOR.

69

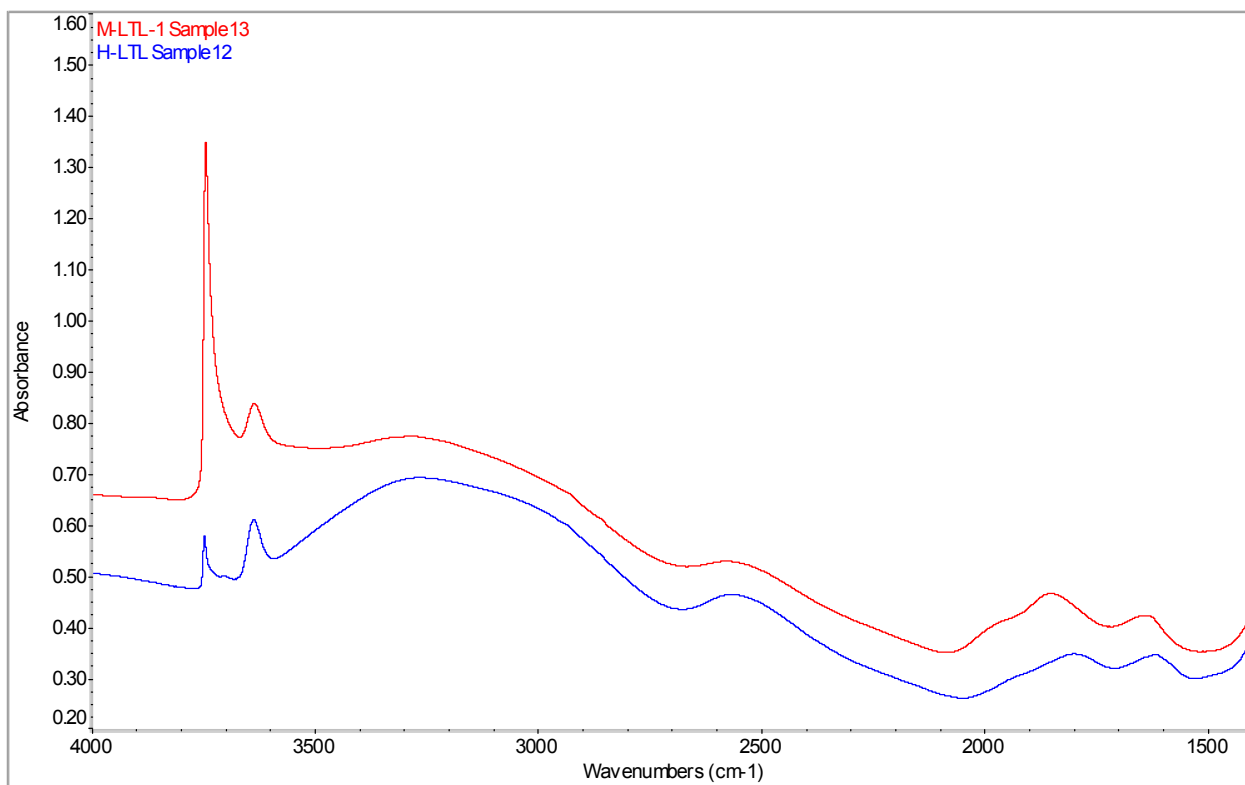


70
 71 **Figure S5c.** FTIR spectra of the O-H region of the **parent (blue)** and **mesostructured (red)** FAU.



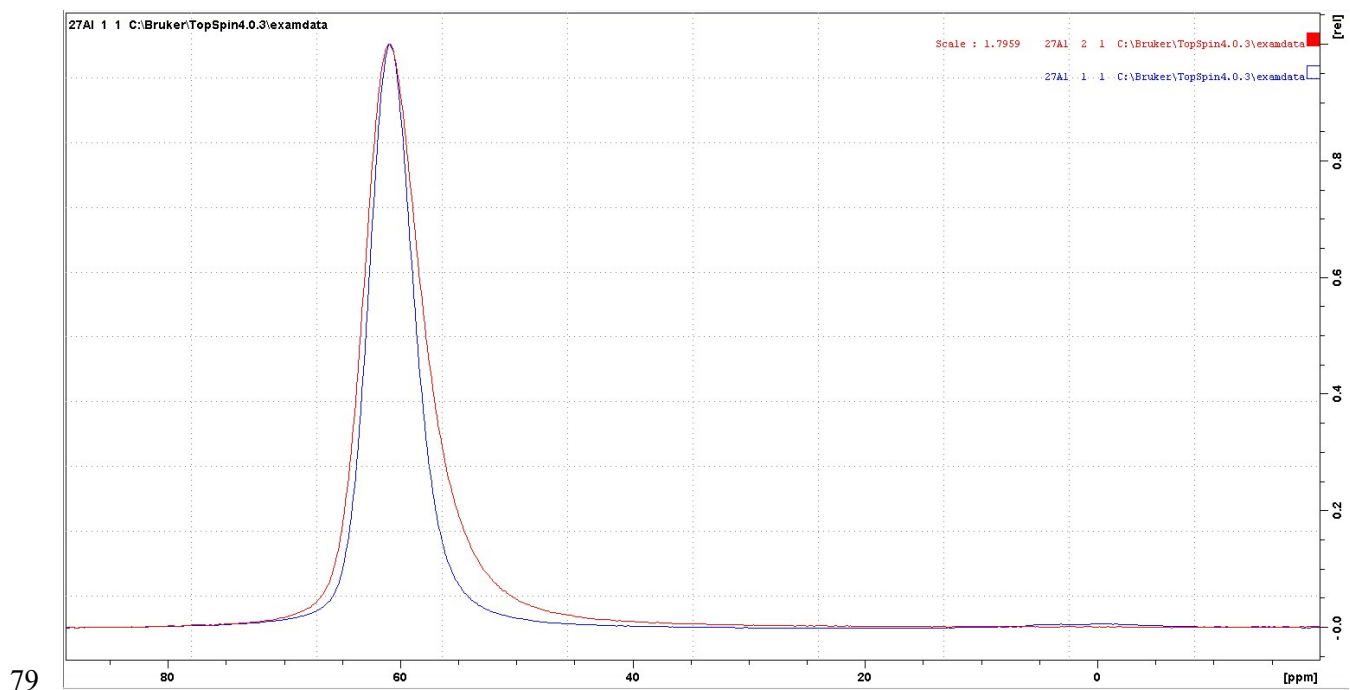
72
 73 **Figure S5d.** FTIR spectra of the O-H region of the **parent (blue)** and **mesostructured (red)** BEA.

74



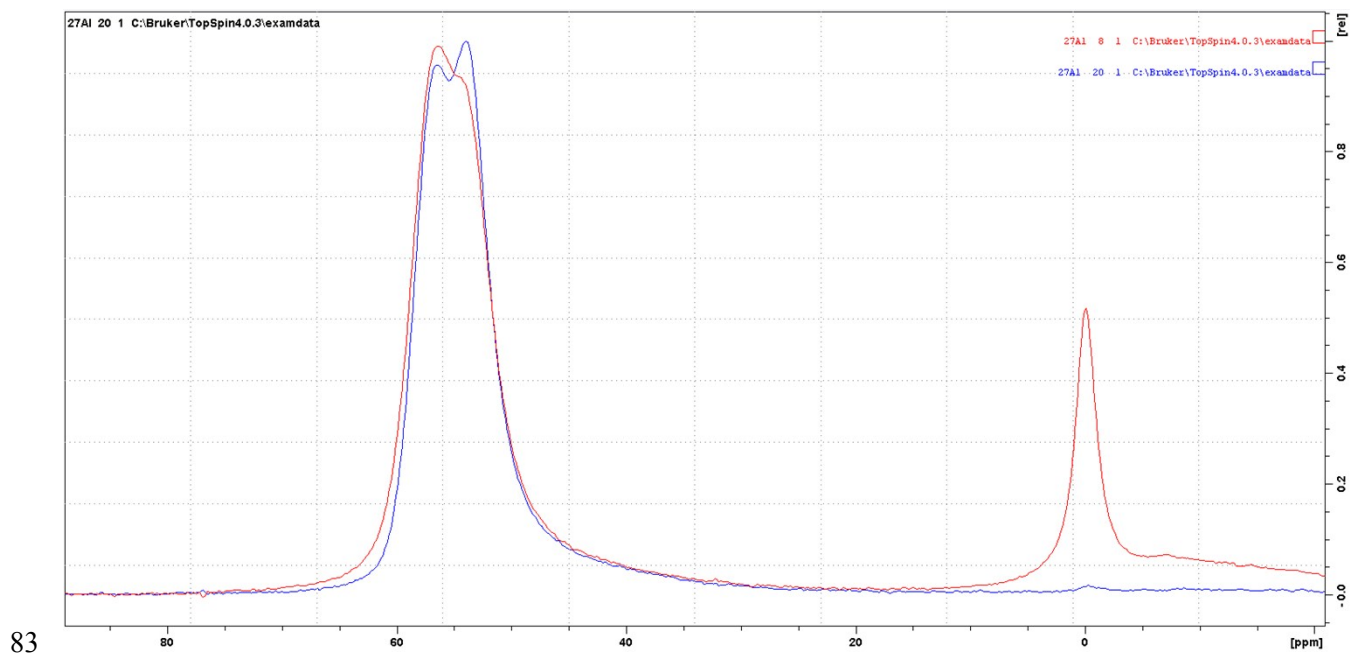
75
 76 **Figure S5e.** FTIR spectra of the O-H region of the **parent (blue)** and **mesostructured (red)** LTL. All
 77 sets of FTIR spectra are offset for clarity.

78



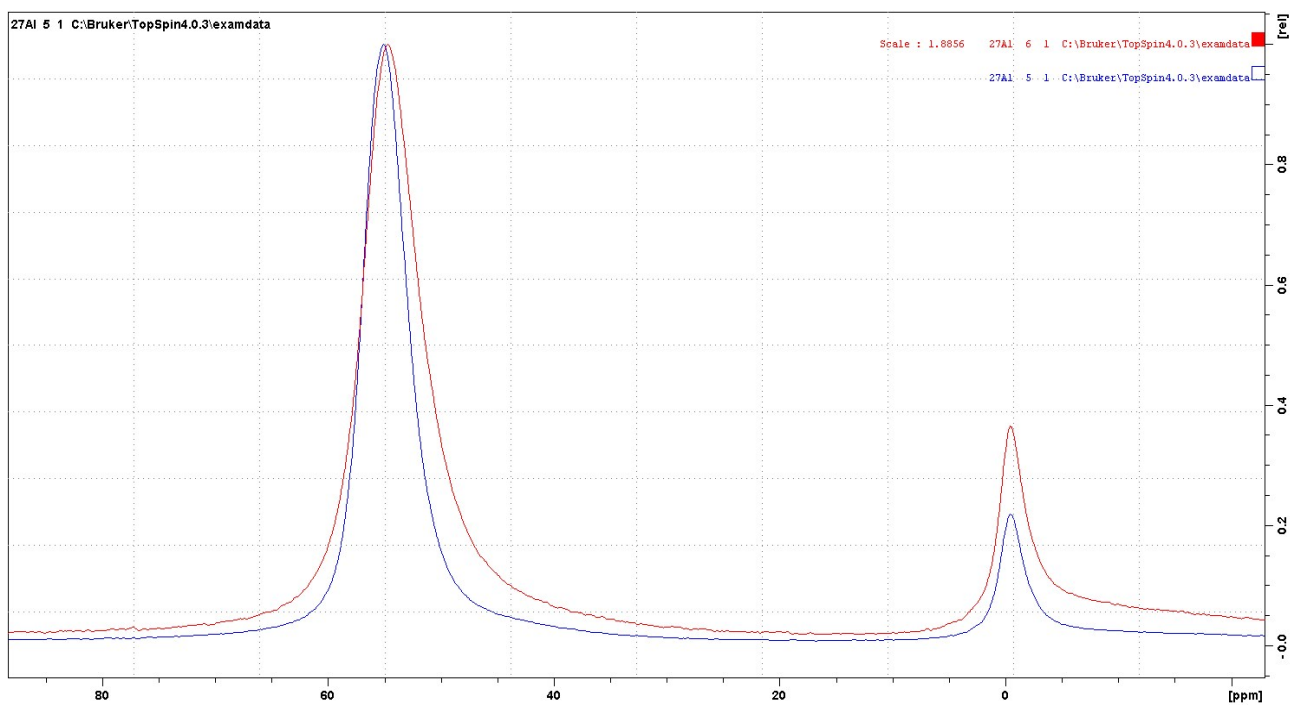
80 **Figure S6a.** ^{27}Al MAS NMR spectra (normalised to the same peak intensity) of the **parent (blue)**
81 and **hierarchical (red)** FAU.

82



84 **Figure S6b.** ^{27}Al MAS NMR spectra (normalised to the same peak intensity) of the **parent (blue)**
85 and **hierarchical (red)** BEA.

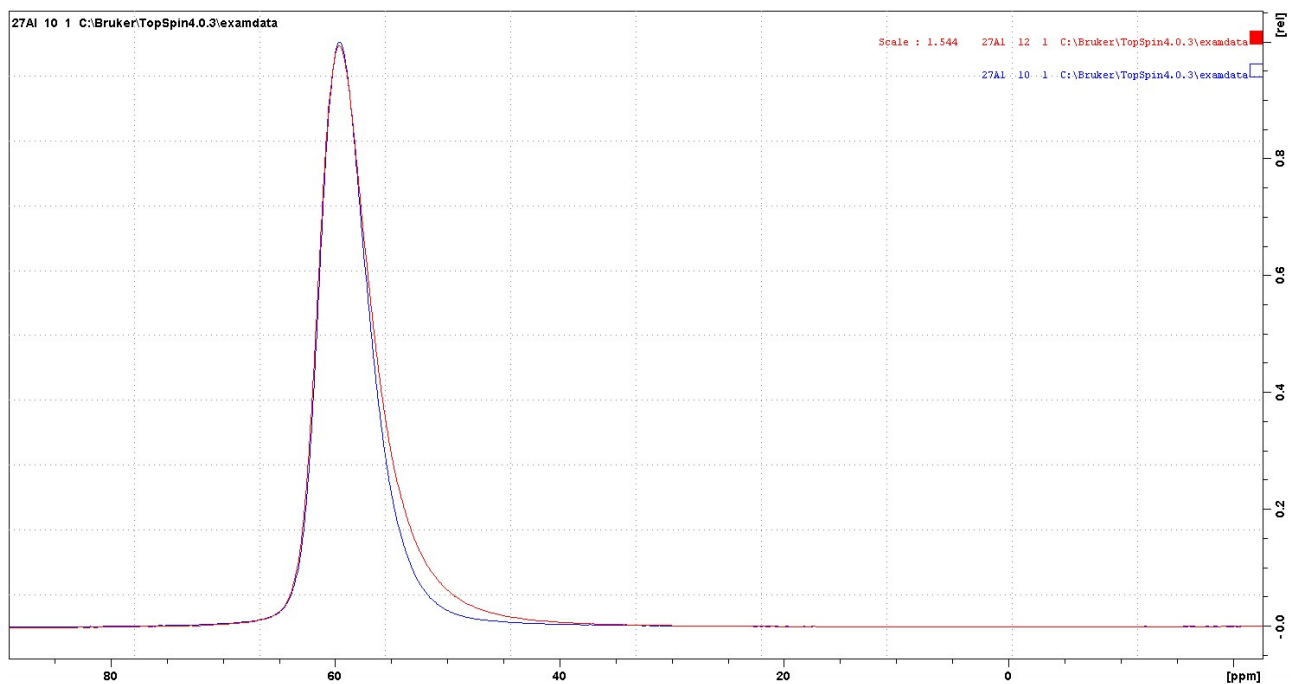
86



87

88 **Figure S6c.** ^{27}Al MAS NMR spectra (normalised to the same peak intensity) of the **parent (blue)**
 89 **and hierarchical (red)** MOR.

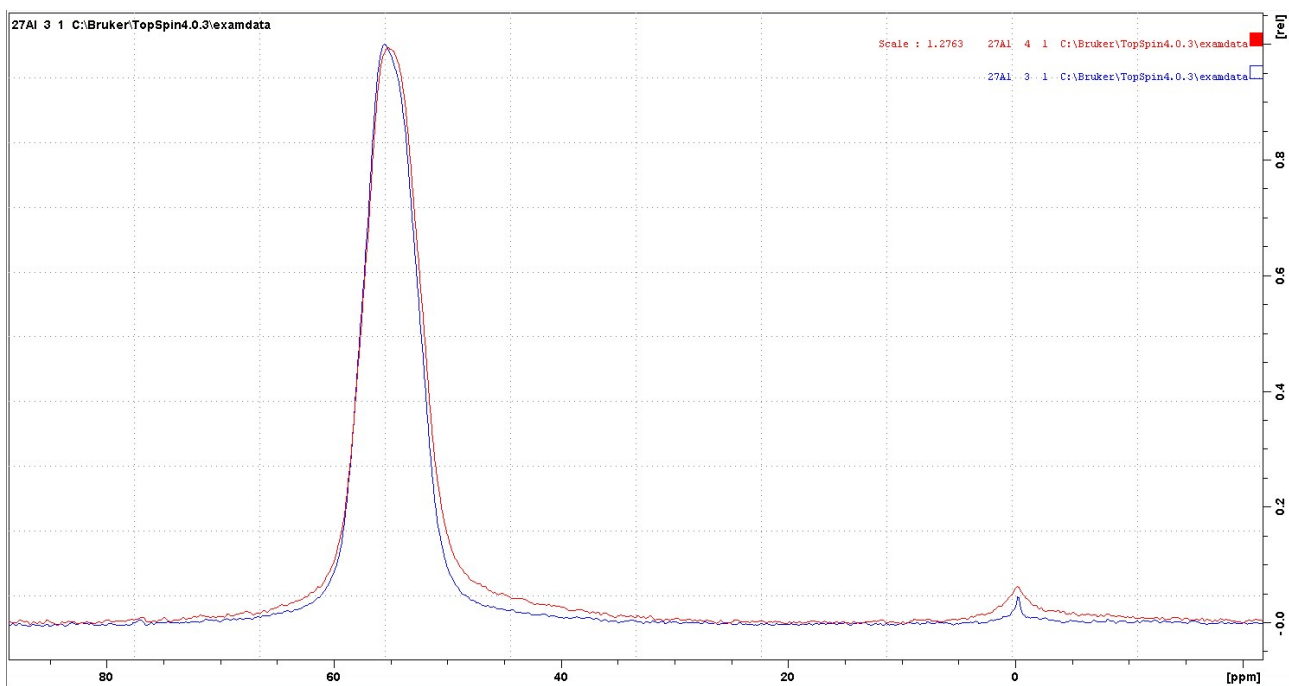
90



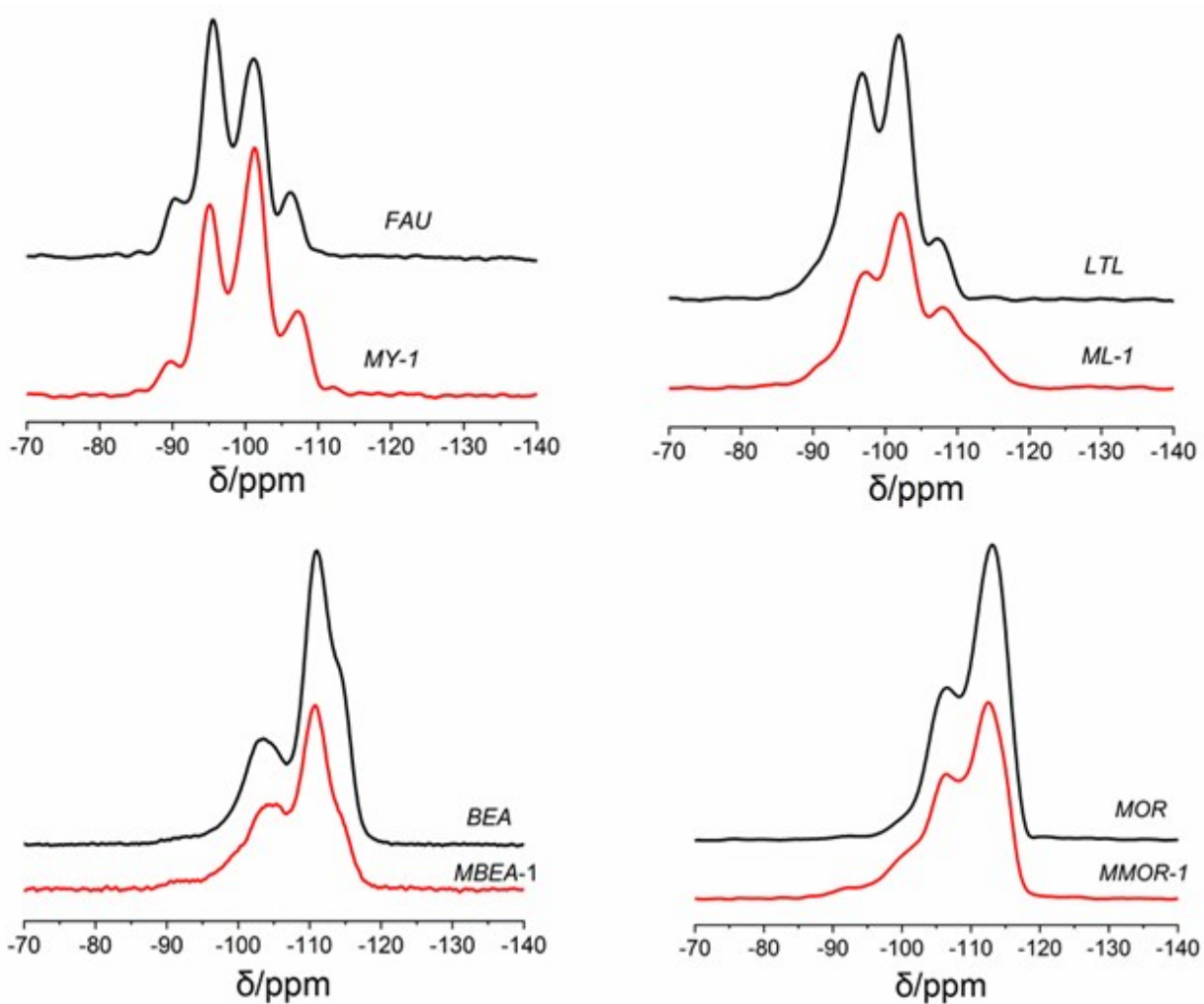
91

92 **Figure S6d.** ^{27}Al MAS NMR spectra (normalised to the same peak intensity) of the **parent (blue)**
 93 **and hierarchical (red)** LTL.

94



95
 96 **Figure S6e.** ^{27}Al MAS NMR spectra (normalised to the same peak intensity) of the **parent** (blue)
 97 and **hierarchical** (red) ZSM-5.



98

99

100 **Figure S7.** ²⁹ Si MAS NMR spectra of the parent and hierarchical zeolites.

101

102 **Table S2. Reaction test data: product selectivities (mol%) and conversion.**

	IPB	MIPB	PIPB	TIPB	Conversion, %
NH4-Y	3%	21%	11%	65%	35%
MY-1	6%	28%	19%	46%	54%
NH4-BEA		8%	4%	88%	12%
MBEA-1		11%	6%	83%	17%
NH4-ZSM-5		2%	0%	98%	2%
MZSM-5-1		6%	0%	94%	6%
NH4-MOR		2%	0%	98%	2%
MMOR-1		7%	3%	91%	9%
NH4-L		1%	0%	99%	1%
ML-1		10%	3%	87%	13%

103 TIPB - 1,3,5-tri-isopropylbenzene

104 IPB - mono-isopropylbenzene

105 MIPB - 1,3- and for all the studied catalysts, and a small amount of

106 PIPB - 1,4-di-isopropylbenzenes